

## Aluminum Dross Use in Metallothermic Ferrochromium Production

Selçuk Yeşiltepe<sup>1</sup>

<sup>1</sup>Selçuk Yeşiltepe Osmaniye Korkut Ata University, Mechanical Eng. Dept., Türkiye

Corresponding author: Selçuk Yeşiltepe, selcukyesiltepe@osmaniye.edu.tr

**Keywords:** Aluminium dross, Ferrochromium, Aluminothermic reduction.

### ABSTRACT

*Aluminum dross contains high amount of metallic Al (up to %60 wt. Al) and regarded as a waste in aluminum casting operations. High metallic value in Al dross can be utilized via recycling procedure. In this study, Al dross was used in aluminothermic ferrochromium production with chromite ore and mill scale. Enthalpy, Gibbs Free Energy and Entropy of reactions calculated via HSC software. Propane-Butane heated furnace was used in the study. Experimental procedure was carried out in a graphite crucible. Effects of stoichiometric ratio of Al and mixing was evaluated in metallization of chromite and mill scale. Results of experimental studies were examined by XRD and SEM/EDS techniques. Results showed that metallization had occurred very limited and further investigations to increase efficiency is mandatory to obtain a fully developed process.*

### 1. INTRODUCTION

Ferrochromium is an essential substance of stainless-steel production as well as tool steels. The type of ferrochromium used in applications depends on the desired end-product. Production of ferrochromium requires high amounts of carbon due to thermodynamic nature of carbothermic reduction of chromite[1]. Carbothermic reduction of chromite ore results in medium or high carbon ferrochromium alloy[1]. On the other hand carbon content of ferrochromium restricts its use in stainless steel production since high amount of carbon is detrimental for corrosion resistance of stainless steel[2]. Low carbon or ultra low carbon ferrochromium are widely used in stainless steel production route[3]. Aluminium is an alternative to carbon in ferrochromium production due to high affinity of aluminium to oxygen[4]. Replacement of carbon with aluminium allows production of low carbon ferrochromium, however use of aluminium instead of carbon based reductants increase the expenditure of process[5-6]. However aluminium dross contains high amounts of metallic aluminium and recycling of aluminium dross is widely applied through the industrial practice[7-12]. Aluminium dross can be successfully utilized in ferrochromium production[10].

In this study aluminium dross, chromite ore and mill scale were used to produce ferrochromium through the aluminothermic process.

### 2. MATERIALS & METHODS

Chromite ore which used in the study was gathered from Elazığ region of Türkiye. Mill scale was provided by a local steel producer. Aluminum dross containing 70% of metallic Al was

obtained from Altınçipa company which produces aluminum alloys in Türkiye. Ferrochromium was produced in a propane-butane heated furnace and temperature was controlled by J-type thermocouple. Temperature was set to 1200 °C and gas flow decreased after reaching desired temperature to conduct experiments. Weighted samples were mixed in a graphite crucible then placed in the furnace. The furnace was heated after the sample was in place.

Chemical composition of chromite ore was given in Table 1. XRD pattern of chromite ore was given in Figure 1.

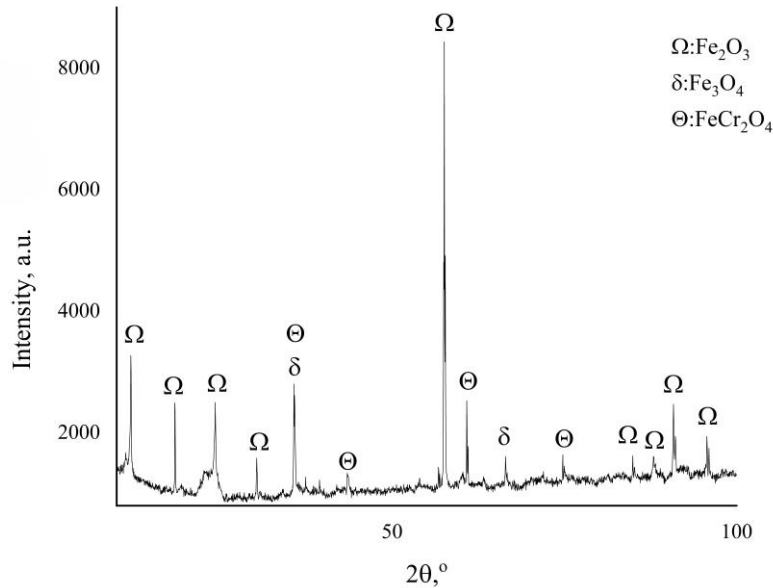


Figure 1. XRD pattern of chromite ore.

Table 1. Chemical composition of Chromite ore.

Substance	Cr <sub>2</sub> O <sub>3</sub>	Fe <sub>2</sub> O <sub>3</sub>	SiO <sub>2</sub>	Al <sub>2</sub> O <sub>3</sub>	Mn <sub>2</sub> O <sub>3</sub>
Weight %	46.712	21.19	7.6718	4.3217	0.328

Chemical composition of mill scale was given in Table 2. XRD pattern of mill scale was given in Figure 2.

Table 2. Chemical composition of mill scale.

Substance	Fe (Total)	MnO	SiO <sub>2</sub>	Cr <sub>2</sub> O <sub>3</sub>	Cu <sub>2</sub> O	Others
Weight %	98.33	0.58	0.21	0.29	0.24	0.15

Chemical composition of Al dross was given in Table 3.

Table 3. Chemical composition of Al dross.

Substance	Al	Al <sub>2</sub> O <sub>3</sub>	SiO <sub>2</sub>	MgO	Others
Weight %	64,38	15,48	1,46	12,37	6,31

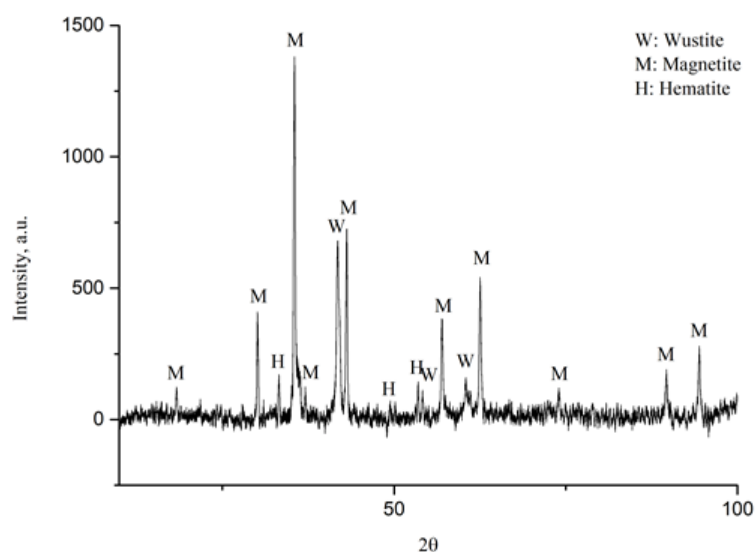


Figure 2. XRD pattern of mill scale.

Thermodynamic calculations were made in HSC 6.1 Thermodynamic Database. Enthalpy, Entropy and Gibbs Free Energy values of reactions were given in Table 4 and Table 5 respectively.

Table 4. Thermodynamic values of  $\frac{1}{2} Fe_2O_3 + Al = \frac{1}{2} Al_2O_3 + Fe$

Temperature, °C	$\Delta H$ , kJ/mol	$\Delta S$ , J/mol K	$\Delta G$ , kJ/mol
500	-431,073	-29,141	-408,543
600	-432,101	-30,391	-405,565
700	-443,756	-42,901	-402,007
800	-442,495	-41,670	-397,777
900	-441,906	-41,142	-393,640
1000	-441,182	-40,521	-389,592
1100	-441,449	-40,723	-385,529
1200	-441,610	-40,837	-381,451

Table 5. Thermodynamic values of  $\frac{1}{2} Cr_2O_3 + Al = \frac{1}{2} Al_2O_3 + Cr$

Temperature, °C	$\Delta H$ , kJ/mol	$\Delta S$ , J/mol K	$\Delta G$ , kJ/mol
500	-274,069	-28,337	-252,160
600	-274,487	-28,846	-249,300
700	-285,536	-40,692	-245,936
800	-285,606	-40,762	-241,862
900	-285,489	-40,659	-237,790
1000	-285,176	-40,404	-233,735
1100	-284,656	-40,012	-229,714
1200	-283,918	-39,494	-225,737

Al dross, chromite ore and mill scale were mixed and prepared for reduction reaction. Mixed raw materials were placed in graphite crucible and placed in furnace. The furnace was ignited and heated then. All reactions took place in ambient conditions for 60 minutes. Used experimental parameters were given in Table 6. 100S/50FC indicates the sample with 100%

stoichiometric Al, non-mixed and 50% FeCr composition. 100SM/50FC indicates the sample with 100% stoichiometric Al, manually mixed and 50% FeCr composition and 150SM/50FC indicates 150% stoichiometric Al, manually mixed and 50% FeCr composition.

Table 6. Experimental Parameters

Sample	Chromite, g	Mill Scale, g	Al Dross, g	Temperature, °C	Time, min	Stoichiometric Ratio of Al, % wt.	Mixing
100S/50FC	100	32.30		1200	60	100	No
100SM/50FC	100	32.30		1200	60	100	Yes
150SM/50FC	100	32.30		1200	60	150	Yes

Reaction results were examined with XRD and SEM/EDS analysis. SEM analyses were conducted via Thermo Fisher Scientific Apreo S SEM. XRD analyses were conducted by Malvern Panalytical Empyrean apparatus using 2 °/min scan speed and 10-110 ° scanning range with Cu K $\alpha$  radiation.

### 3. RESULTS & DISCUSSION

XRD result of experiments was given in Figure 3. XRD result showed that main structure of reduced ore was in oxide form. Overlapping of metallic and oxide phases X-ray diffraction caused peak shifts in XRD pattern. Due to this phenomenon strongest match of all peaks were selected.

Figure 3. XRD pattern of reduction experiments.

Rietveld analysis of samples was not conducted due to large amounts of different compounds in the XRD pattern. Rietveld analysis in the standard mode were unable to calculate phases.

SEM/EDS analyses of samples were done for each reduction condition. Images of 100S/50FC SEM samples were given in Figure 4 with EDS results in Table 7. Point 4 of EDS result showed metallization of mainly Fe. Aluminothermic reduction of Fe is more favorable to Cr according to thermodynamic calculations. However, metallization was seen in a very limited area.

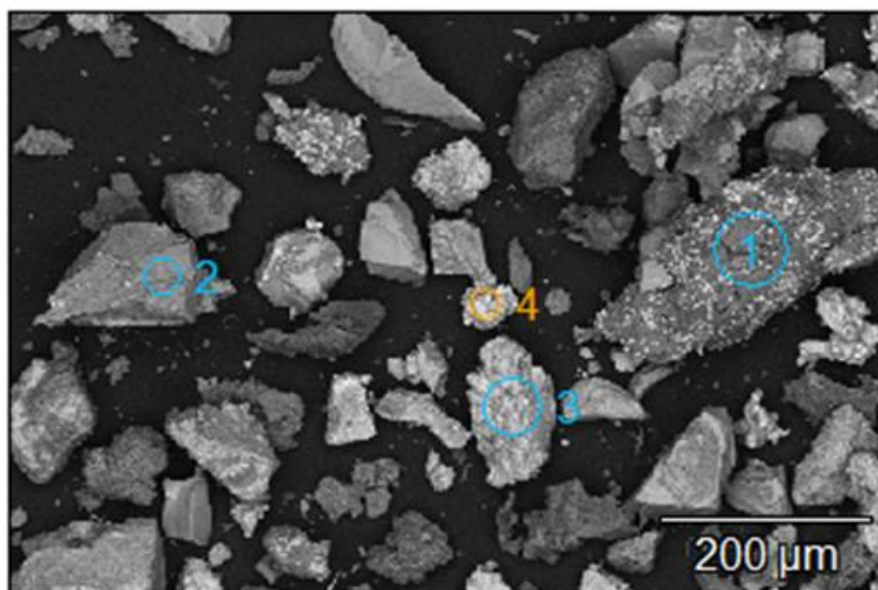


Figure 4. SEM image of 100S/50FC sample.

Table 7. EDS results of 100S/50FC sample.

Point	O, wt. %	Fe, wt. %	Cr, wt. %	Al, wt. %	Mg, wt. %	Si, wt. %
1	27,22	28,29	4,21	0,63	25,98	13,67
2	25,57	19,80	32,95	5,43	12,28	3,97
3	16,64	68,65	5,98	5,59	2,40	0,74
4	3,15	87,49	2,83	1,87	3,72	0,94

Images of 100SM/50FC SEM samples were given in Figure 5 with EDS results in Table 8. Results were similar to 100S/50FC sample. Metallic particles were accumulated on ore particles.

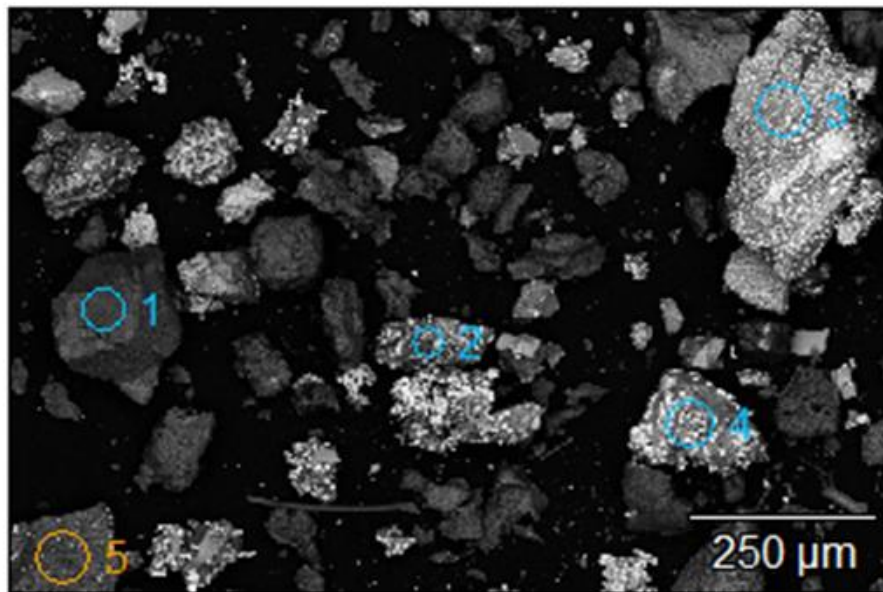


Figure 5. SEM image of 100SM/50FC sample.

Table 8. EDS results of 100SM/50FC sample.

Point	O, wt. %	Fe, wt. %	Cr, wt. %	Al, wt. %	Si, wt. %
1	33.30	1,47	0,34	64,89	-
2	11.04	63,14	21,22	1,06	3,53
3	20.79	52,76	21,84	3,72	0,90
4	26.43	42,83	20,02	4,38	6,34
5	44.48	23,03	1,19	4,35	26,95

150SM/50FC sample was examined with same procedure. Results showed similar results with other samples. Results were given in Figure 6 and Table 9.

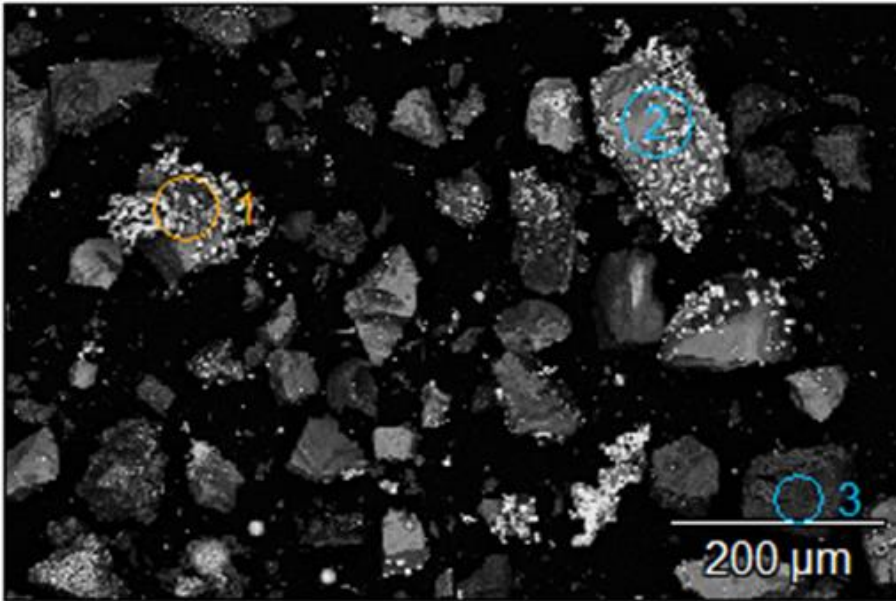


Figure 6. SEM image of 150SM/50FC sample.

Table 9. EDS results of 150SM/50FC sample.

Point	O, wt. %	Fe, wt. %	Cr, wt. %	Al, wt. %	Si, wt. %	Mg, %
1	15,82	51,24	11,87	2,17	5,77	13,12
2	18,62	45,92	22,95	3,91	1,56	7,04
3	43,45	7,08	1,13	0,60	18,49	29,25

Detailed SEM image and EDS analysis of 150SM/50FC sample was conducted. Results showed that bright particles on larger dark particles had lower amounts of Oxygen and metallization occurred in these regions. It was understood that larger dark particles indicate chromite ore or mill scale while bright smaller particles indicating metallization zones. Detailed SEM image with EDS analysis were given in Figure 7 and Table 10 respectively.

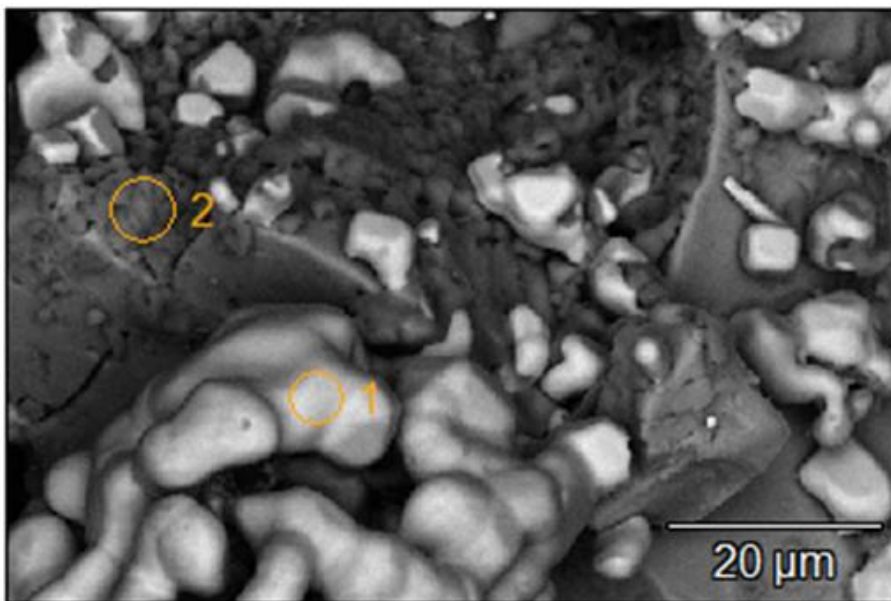


Figure 7. Detailed SEM image of 150SM/50FC sample.

Table 10. EDS results of 150SM/50FC sample.

Point	O, wt. %	Fe, wt. %	Cr, wt. %	Al, wt. %	Si, wt. %	Mg, %
1	3,43	94,35	1,50	0,50	0,10	0,12
2	35,85	13,57	19,20	4,06	8,66	18,66

All results combined it was concluded that metallization of chromite ore and mill scale occurred on oxide particles with solid-solid interaction. Solid-solid reactions are kinetically slow, requiring more time and energy to be completed. Solid state production of ferrochromium was unsuccessful, and metallization was very limited. Increasing stoichiometric ratio of Al and manual mixing of charge increased the metallization.

#### 4. CONCLUSION

Solid state reduction of chromite ore with mill scale to produce 50% wt. FeCr was studied with Al dross as reductant. Results were examined with XRD, SEM and EDS analyses. Results combined demonstrated that reduction reaction occurred on ore particles with solid-solid and solid-liquid interaction zone. Limited contact area restricted mass reduction of chromite. Mixing of charge increased the contact area of reactants thus increasing in metallization. 150% stoichiometric Al showed better results by mean of metallization.

Thermodynamic calculations showed possibility of solid-state reduction of chromite however kinetic restrictions of solid-state reduction decreased the metallization rate. Density difference between Al and ores requires automated mix of the charge. Higher Al content, automated mixing of charge and increase in temperature would be helpful to obtain higher metallization rates. Wetting angle of Al on chromite particles should be investigated for further development of process. Start of metallization is a promising feature to further investigations of Al dross use in metallothermic reactions.

#### 5. REFERENCES

- [1] M. Eissa and H. El-Farmawy, 'Carbothermic smelting of high carbon ferrochromium alloy from low and high grade chromite ores', *Ironmak. Steelmak.*, vol. 39, no. 1, pp. 31–37, Jan. 2012, doi: 10.1179/1743281211Y.0000000047.
- [2] Q. Kou, W. Jin, G. Liu, M. Wang, and S. Xiao, 'Electrolytic Refining of High Carbon Ferrochromium to Produce Pure Ferrochromium in NaCl-KCl Melt', *Int. J. Electrochem. Sci.*, vol. 14, no. 9, pp. 8557–8568, Sep. 2019, doi: 10.20964/2019.09.05.
- [3] D. K. Isin *et al.*, 'Ferrochromium Smelting Technology', *Metallurgist*, vol. 57, no. 7–8, pp. 682–689, Nov. 2013, doi: 10.1007/s11015-013-9787-9.
- [4] B. M. Wenzel, T. H. Zimmer, C. S. Fernandez, N. R. Marcilio, and M. Godinho, 'Aluminothermic reduction of Cr<sub>2</sub>O<sub>3</sub> contained in the ash of thermally treated leather waste', *Braz. J. Chem. Eng.*, vol. 30, no. 1, pp. 141–154, Mar. 2013, doi: 10.1590/S0104-66322013000100016.
- [5] B. M. Wenzel, T. H. Zimmer, C. S. Fernandez, N. R. Marcilio, and M. Godinho, 'Aluminothermic reduction of Cr<sub>2</sub>O<sub>3</sub> contained in the ash of thermally treated leather waste', *Braz. J. Chem. Eng.*, vol. 30, no. 1, pp. 141–154, Mar. 2013, doi: 10.1590/S0104-66322013000100016.
- [6] A. R. Kachin, V. E. Loryan, and I. P. Borovinskaya, 'Aluminothermic SHS of ferrochromium from ore concentrate: Influence of Al content of green composition on phase segregation', *Int. J. Self-Propagating High-Temp. Synth.*, vol. 25, no. 1, pp. 59–61, Jan. 2016, doi: 10.3103/S1061386216010052.
- [7] J. Gottmyers Melwyn, B. Chandragandhi, G. Sathiyaseelan, and P. Srinath, 'Aluminium scrap recycling in a production furnace: Minimizing dross formation for sustainable and efficient

- recovery', *Mater. Today Proc.*, p. S2214785323029760, May 2023, doi: 10.1016/j.matpr.2023.05.340.
- [8] K. Modalavalasa and K. P. R. Ayyagari, 'Aluminum dross: aluminum metal recovery and emerging applications', *J. Mater. Cycles Waste Manag.*, vol. 26, no. 4, pp. 1874–1894, Jul. 2024, doi: 10.1007/s10163-024-01948-0.
- [9] L. Xueqin *et al.*, 'Feasibility assessment of recycling waste aluminum dross as a basic catalyst for biomass pyrolysis to produce hydrogen-rich gas', *Int. J. Hydrog. Energy*, vol. 48, no. 93, pp. 36361–36376, Dec. 2023, doi: 10.1016/j.ijhydene.2023.06.049.
- [10] A. Srivastava and A. Meshram, 'On trending technologies of aluminium dross recycling: A review', *Process Saf. Environ. Prot.*, vol. 171, pp. 38–54, Mar. 2023, doi: 10.1016/j.psep.2023.01.010.
- [11] M. Kale, İ. H. Yılmaz, A. Kaya, A. E. Çetin, and M. S. Söylemez, 'Pilot-scale hydrogen generation from the hydrolysis of black aluminum dross without any catalyst', *J. Energy Inst.*, vol. 100, pp. 99–108, Feb. 2022, doi: 10.1016/j.joei.2021.11.005.
- [12] S. K. Verma, V. K. Dwivedi, and S. P. Dwivedi, 'Utilization of aluminium dross for the development of valuable product – A review', *Mater. Today Proc.*, vol. 43, pp. 547–550, 2021, doi: 10.1016/j.matpr.2020.12.045.